Cilt 11, Sayı 4, Sayfa 104-110, 2022

Volume 11, Issue 4, Page 104-110, 2022

Araştırma Makalesi https://doi.org/10.46810/tdfd.1199583 Research Article

Türk Doğa ve Fen Dergisi
Turkish Journal of Nature and Science
www.dergipark.gov.tr/tdfd

$Wb\bar{b}$ QCD Predictions in Proton Proton Collisions for the LHC and FCC

Kamuran DİLSİZ[1*]

[1]Bingol University, Art and Science Faculty, Physics Department, Bingöl, Türkiye
Kamuran DİLSİZ ORCID No: 0000-0003-0138-3368

**Corresponding author: kdilsiz@bingol.edu.tr*

(Received: 04.11.2022, Accepted: 05.12.2022, Online Publication: 28.12.2022)

Keywords
QCD,
LHC,
FCC,
W Boson,
b quark.

Abstract: This study presents leading order (LO) and next-to-leading order (NLO) QCD cross sections for inclusive $Wb\bar{b}$ production channel at 14, 27 and 100 TeV center-of-mass energies for the Large Hadron Collider (LHC) and Future Circular Collider (FCC). To obtain the numerical results, five modern parton distribution functions (PDFs) were used and the PDF errors were obtained by the MCFM Monte Carlo program. In addition, a scale uncertainty calculation was performed for different values of renormalization and factorization scales. Contrary to the single W channel scale uncertainty results, the scale uncertainties in NLO QCD were found to be higher than the scale uncertainties in LO QCD for all energies considered in this calculation. To show the effect of the increasing energy on the uncertainties, a comparison of the scale, PDF and α_S uncertainties with the increasing energy were performed. To confirm the consistency of the code used in the current study, a comparison of the Monte Carlo results at $\sqrt{s}$ =7 TeV were performed with the available CMS data at the same energy. Then, LO and NLO QCD cross sections of $Wb\bar{b}$ production channel at $\sqrt{s}$ =14, 27 and 100 TeV were calculated. Using these results, the required amount of data that reach the same statistics with $\sqrt{s}$ =7 TeV energy were calculated for $\sqrt{s}$ = 14, 27 and 100 TeV energies.

Proton Proton Çarpışması Sonucu Oluşan $Wb\bar{b}$ Üretim Kanalının LHC ve FCC İçin Kuantum Renk Dinamiği Tahminleri

Anahtar Kelimeler
QCD,
LHC,
FCC,
W Boson,
b quark.

Öz: Bu çalışma, Büyük Hadron Çarpıştırıcısı (BHÇ) ve Gelecekteki Dairesel Çarpıştırıcı (FCC) için 14, 27 ve 100 TeV kütle merkez enerjilerinde $Wb\bar{b}$ üretim kanalının leading order (LO) ve next-to-leading order (NLO) kuantum renk dinamiği (KRD) tesir kesitlerini sunmaktadır. Sayısal sonuçları elde etmek için beş farklı parton dağılım fonksiyonu (PDF) kullanılmış ve PDF hataları MCFM Monte Carlo programı ile elde edilmiştir. Ayrıca renormalizasyon ve faktörizasyon ölçeklerinin farklı değerleri için scale hata payı hesaplaması yapılmıştır. W üretim kanalında elde edilen scale hata paylarının aksine $Wb\bar{b}$ üretim kanalında NLO QCD'deki scale hata payları LO QCD'deki scale hata paylarından daha yüksek bulunmuştur. Artan enerjinin hata payları üzerindeki etkisini test etmek için, artan enerji ile scale, PDF ve α_S belirsizliklerinin karşılaştırılması yapılmıştır. Ayrıca, bu çalışmada kullanılan simülasyon kodunun doğruluğunu onaylamak için $\sqrt{s}$ =7 TeV enerji değerinde elde edilen sonuçlar ile aynı enerjideki CMS verileri karşılaştırılmıştır. Yazılmış olan kodların doğruluğunun onaylanmasından sonra, $Wb\bar{b}$ üretim kanalının $\sqrt{s}$ = 14, 27 ve 100 TeV'deki LO ve NLO QCD tesir kesitleri hesaplanmıştır. Daha sonra $\sqrt{s}$ = 7 TeV enerjisindeki veri ile aynı istatistiğe sahip verinin elde edilmesi için $\sqrt{s}$ = 14, 27 ve 100 TeV enerjilerinde ihtiyaç duyulan veri miktarı hesaplanmıştır.

1. INTRODUCTION

Particle accelerators are huge colliders that play significant roles in search of new particles in high energy and particle physics. Particularly, the necessity of testing various predicted theories in the Standard Model (SM) and beyond it has increased the necessity for particle accelerators. The Large Hadron Collider (LHC) [1], the current largest accelerator in the world, focuses on new discoveries and searches for new physics. The LHC was initially operated at 7 TeV center-of-mass energy ($\sqrt{s}$) in

2009 and the energy was increased to 8 TeV in 2012. It is currently operating at 13.8 TeV and the energy will reach its desired collision energy of 14 TeV in the near future. Luminosity, the number of collisions per centimeter square per second, that occur in particle colliders, is an important parameter that shows the accelerator's performance. Higher luminosity provides more data to observe rare processes. To increase the performance of the LHC with a luminosity increase, High-Luminosity LHC (HL-LHC) has been planned to operate at 14 TeV with 10 times higher luminosity than that of the current run [2].

The likelihood high energy colliders that are planned to build in the future will contribute to search new physics. Comparing to the current colliders, they will provide the opportunity of testing theoretical predictions that cannot be estimated at low energies because of their high energies. The Future Circular Collider (FCC), which is planned to be built at CERN with a maximum 100 TeV collision energy, is projected to have three accelerators according to its conceptual design report. These are FCC-ee (electron-positron), High-Energy LHC (HE-LHC) and FCC-hh collider (proton-proton, ion-ion) [3]. The beams of electron and positron at several center-of-mass energies will be collided at FCC-ee [4]. After HL-LHC has successfully finished its operation, the beams of protons at $\sqrt{s}$= 27 TeV will be collided at HE-LHC [5] which will be located in the same tunnel with the LHC. The proton beams at $\sqrt{s}$= 100 TeV will be collided at FCC-hh collider [6] and this energy will be the maximum planned energy of the collider.

Understanding of the detectors and their response to the particles produced is required for the measurement of the proposed signals of the processes that provide access to new physics. A precise software calibration depends on accurate calculation of the cross-section processes of particles whose properties are well known. QCD predictions, that are very important in determining the cross section of a particle, is calculated by the monte carlo production tools. MCFM [7] monte carlo program is one of these tools and it produces the QCD results of many physics processes. In this context, we have calculated LO and NLO QCD cross sections of $Wb\bar{b}$ production channel using MCFM program. Parton distribution functions (PDFs), which give the probability to find partons in a hadron, are important parameters to calculate the cross sections of the physics processes produced by the hadron colliders. Therefore, we used LHAPDF6 [8] library to select different PDFs for calculation.

The total and differential cross sections of $Wb\bar{b}$ at 10 TeV and 14 TeV center-of-mass energies were previously calculated [9]. However, our purpose in this study is not to follow the same steps that were provided in Ref [9]. In current study, $Wb\bar{b}$ LO and NLO QCD predictions were obtained at $\sqrt{s}$ = 27 TeV and 100 TeV in addition to $\sqrt{s}$ = 14 TeV. Additionally; scale, PDF and α_S uncertainties were calculated and the effect of increasing energy on the uncertainties were provided. Particularly, using two different methods in the selection of renormalization (μ_R) and factorization (μ_F) scales, the scale uncertainties were calculated (section 3.1). All results were produced by the MCFM monte carlo program [7] and five modern PDFs were used to confirm the selection of the reference PDF (NNPDF3.1). In the last step, the necessary amount of data at $\sqrt{s}$ = 14, 27 and 100 TeV energies were calculated to show the amount of data to reach the same statistic with the data at $\sqrt{s}$ = 7 TeV (section 3.2).

2. GENERAL SETUP

In this study, the results of $Wb\bar{b}$ production channel were obtained both for the next LHC run and FCC pp collider runs. The production energies have been set to 14 TeV and 27 TeV (100 TeV) center-of-mass energy for the LHC and the HE-LHC (FCC-hh), respectively. The focus of the study was the leptonic decay of the W boson. The mass of the b quark was taken as m_b = 4.62 GeV. Because of the geometry in the detectors of the LHC (CMS and ATLAS), the selection criteria were set on the lepton transverse momentum (p_T^l) and lepton pseudorapidity (η). For this channel, a p_T^l greater than 25 GeV was preferred and η value of leptons and b jets smaller than 2.5 were selected. Having the pseudocone size (R) equal to 0.7, the $k_T$algorithm [10, 11] was implemented for the b jets. μ_R and μ_F scales were selected as μ_R= μ_F=$M_W + 2M_b$ where M_W and M_b are the masses of the W and b quarks, respectively . The scale uncertainty was calculated taking the differences between the cross section values of twice and half of the default μ_R and μ_F. More details about the calculation of the scale uncertainty implemented in this study is given in our previous study [12]. Following the confirmation of the NNPDF3.1 PDF through the comparison of five different PDF sets, both the LO and NLO predictions were obtained with the NNPDF3.1 PDF set [13]. The strong coupling factor, α_S (M_Z), was set to 0.118 both for LO and NLO QCD corrections.

3. RESULTS AND DISCUSSIONS

3.1. Uncertainties

The uncertainties calculated in this study were obtained based on the chosen reference PDF, NNPDF3.1.To search the effect of increasing collision energy on the rank of the uncertainties; PDF, scale and α_S uncertainties were computed at $\sqrt{s}$ = 14, 27 and 100 TeV energies respectively by taking the LO and NLO accuracies of the cross sections into account. PDF uncertainties were calculated following the steps defined at ref. [20]. Varying the values of μ_R and μ_F, two different scale uncertainties were calculated. Initially, the masses of the W boson and b quarks were taken into account and the μ_R and μ_F were simultaneously varied as $\frac{M_{W+2b}}{2} \leq \mu_R \leq 2M_{W+2b}$ and $\frac{M_{W+2b}}{2} \leq \mu_F \leq 2M_{W+2b}$ (scale 1), where M_{W+2b} is the sum of W boson and b quarks masses. Then, the mass of W boson was taken into account and the μ_R and μ_F simultaneously varied as $\frac{M_W}{2} \leq \mu_R \leq 2M_W$ and $\frac{M_W}{2} \leq \mu_F \leq 2M_W$ (scale 2), where M_W is the mass of W boson.

The default values of μ_R and μ_F were set to M_{W+2b} and M_W for scale 1 and scale 2, respectively. Then, the variations were assigned as up and down errors. In order to calculate α_S error, α_S was varied by 0.002 and the difference with the default value was taken as α_S error. The numerical results of the calculated LO (NLO) uncertainties are given in Table 1 (Table 2). A comparison of the scale 1, scale 2, PDF and α_S errors are shown in Figure 1. NLO QCD suffers from scale uncertainty even though the scale uncertainty shows low systematic error at LO QCD. In addition, all uncertainties increase with the increasing energy at LO and NLO QCD except of the scale uncertainty at $\sqrt{s}$ = 100 TeV at LO QCD. These results show that the scale uncertainty at next runs (14, 27 and 100 TeV) will suffer with high systematic errors. In order to reduce the uncertainty, higher order calculations would be necessary.

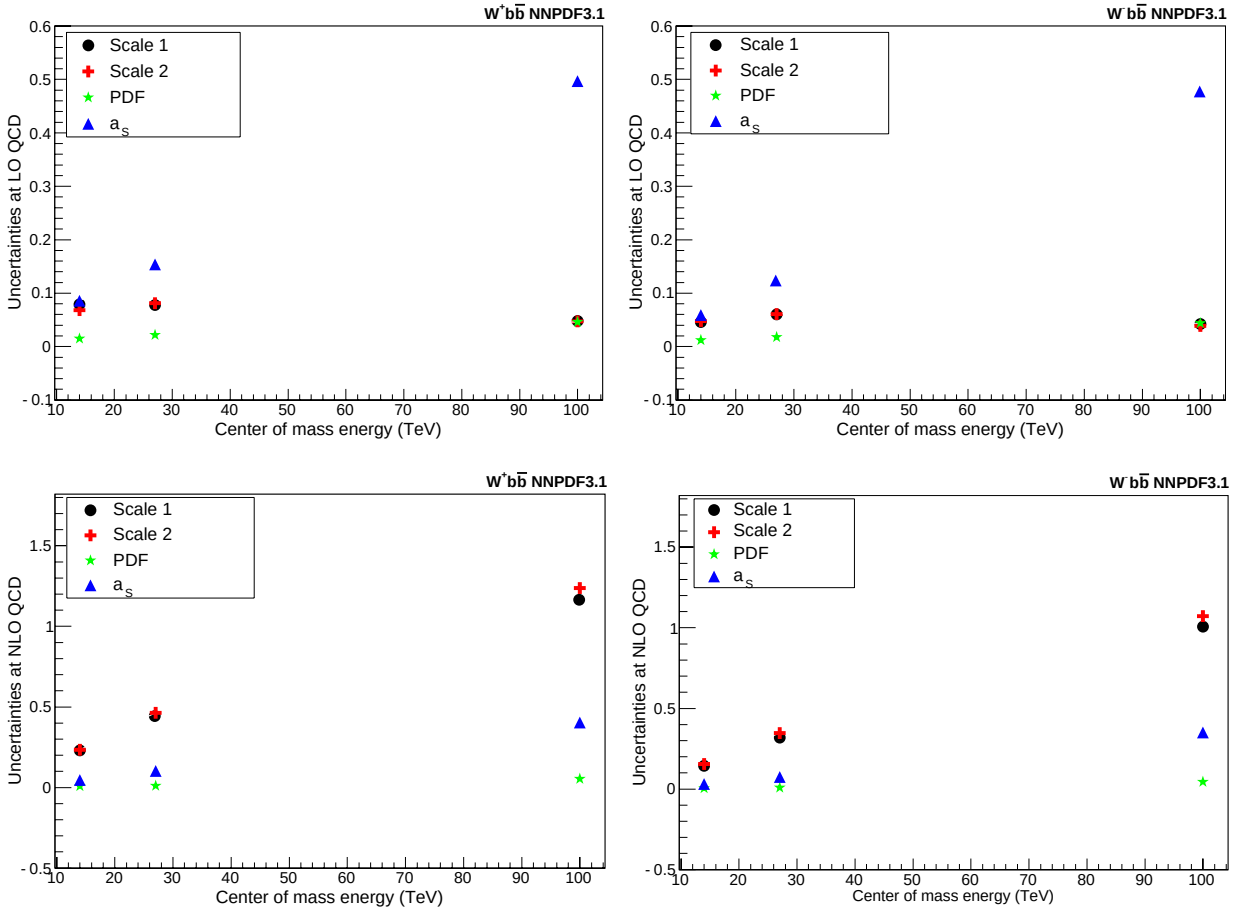

Figure 1. Scale, PDF and α_S uncertainties at LO and NLO QCD for $W^+b\bar{b}$ (left) and $W^-b\bar{b}$ (right) production channel.

Table 1. The numerical results of the uncertainties calculated at LO QCD for different energies. All results are in the units of pb.

Production Channel	Uncertainty	14 Tev	27 TeV	100 TeV
$W^+b\bar{b}$	Scale 1	+0.079 −0.053	+0.078 −0.067	+0.033 −0.048
	Scale 2	+0.068 −0.056	+0.081 −0.070	+0.037 −0.047
	PDF	+0.015 −0.015	+0.022 −0.022	+0.046 −0.046
	α_S	+0.086 −0.086	+0.154 −0.154	+0.497 −0.497
$W^-b\bar{b}$	Scale 1	+0.046 −0.037	+0.060 −0.053	+0.024 −0.042
	Scale 2	+0.048 −0.038	+0.061 −0.054	+0.025 −0.039
	PDF	+0.012 −0.012	+0.018 −0.018	+0.044 −0.044
	α_S	+0.059 −0.059	+0.123 −0.123	+0.476 −0.476

Table 2. The numerical results of the uncertainties calculated at NLO QCD for different energies. All results are in the units of pb.

Production Channel	Uncertainty	14 Tev	27 TeV	100 TeV
$W^+b\bar{b}$	Scale 1	+0.226 −0.163	+0.441 −0.321	+1.162 −0.950
	Scale 2	+0.234 −0.170	+0.463 −0.335	+1.238 −0.953
	PDF	+0.008 −0.008	+0.011 −0.011	+0.053 −0.053
	α_S	+0.046 −0.047	+0.102 −0.094	+0.404 −0.367
$W^+b\bar{b}$	Scale 1	+0.144 −0.105	+0.318 −0.235	+1.006 −0.837
	Scale 2	+0.155 −0.112	+0.347 −0.240	+1.073 −0.850
	PDF	+0.005 −0.005	+0.008 −0.008	+0.045 −0.045
	α_S	+0.032 −0.031	+0.075 −0.073	+0.351 −0.345

3.2. QCD Predictions at $\sqrt{s}$ = 14, 27 and 100 TeV

CMS collaboration previously measured inclusive $Wb\bar{b}$ fiducial cross section with the data taken by the CMS detector at 7 TeV center-of-mass energy [14]. Since we make the predictions for the future experiments and have no available experimental data at $\sqrt{s}$ = 14, 27 and 100 TeV, the confirmation of the codes used in the MCFM program are crucial in terms of obtaining the accurate results for the future experiments. These were verified through comparison of the fiducial QCD predictions of $Wb\bar{b}$ at $\sqrt{s}$= 7 TeV with the results obtained by the CMS collaboration at the same energy. Using the selection criteria explained in section 2, LO and NLO QCD predictions were obtained by the MCFM and the predicted results are given in Table 3. The comparison of the LO and NLO QCD predictions with the experimental CMS results are illustrated in Figure 2. NLO prediction is consistent with the data while the LO prediction does not agree with the experimental results. Since the NLO accuracy has one loop matrix element, it provides more accurate calculations in comparison to the LO correction. Due to this, NLO QCD results show a better agreement with the experimental data. This confirmation shows the validation of the codes in the MCFM for the next runs at higher energies ($\sqrt{s}$ = 14, 27 and 100 TeV). However, selection of an appropriate PDF among the most modern ones are needed as there are differences among the PDF groups. This study has compared the NLO QCD predictions obtained by NNPDF3.1 with the NLO corrections obtained by CT14 [15], MSTW2008 [16, 17], MMHT2014 [18] and HERA [19] PDFs (Fig. 3). This comparison shows that the results obtained by NNPDF3.1 are consistent with the outcomes of the other PDFs. This confirmed the reliability of NNPDF3.1 comparing its results with the results obtained by the other PDFs (Fig. 3). The numerical results of NLO QCD predictions obtained with different PDFs for $W^+b\bar{b}$ and $W^-b\bar{b}$ production channels at $\sqrt{s}$ = 14, 27 and 100 TeV are given in Table 4. According to the results given in table 4, NNPDF3.1 results at $\sqrt{s}$ =14 TeV in $W^+b\bar{b}$ ($W^-b\bar{b}$) channel are respectively 1.61% (0.75%), 2.45% (4.42%), 2.83% (3.32%) and 1.00% (1.47%) different than CT14, MSTW2008, MMHT2014 and HERA PDF results. In addition, NNPDF3.1 results at $\sqrt{s}$ =27 TeV in $W^+b\bar{b}$ ($W^-b\bar{b}$) channel are respectively 1.65% (1.64%), 2.19% (4.30%), 2.83% (3.60%) and 1.77% (3.00%) different than CT14, MSTW2008, MMHT2014 and HERA PDF results. Moreover, NNPDF3.1 results at $\sqrt{s}$ =100 TeV in $W^+b\bar{b}$ ($W^-b\bar{b}$) channel are respectively 1.82% (1.91%), 2.49% (3.38%), 2.92% (3.03%) and 4.72% (4.74%) different than CT14, MSTW2008, MMHT2014 and HERA PDF results.

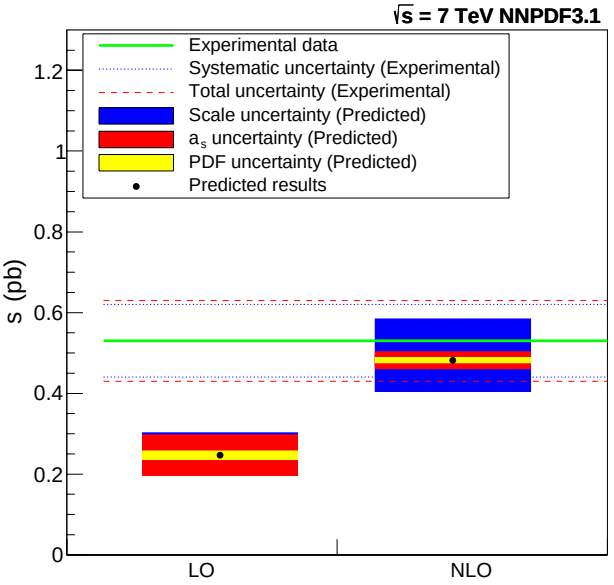

Figure 2. A comparison of LO and NLO QCD results obtained by NNPDF3.1 PDF with the data taken by the CMS detector at $\sqrt{s}$ = 7 TeV.

Table 3. LO and NLO QCD predictions for $Wb\bar{b}$ production channel at $\sqrt{s}$ = 7 TeV. The uncertainties are respectively scale, α_S, and PDF errors. All results are in the units of pb.

Production Channel	LO	NLO
$W^+b\bar{b}$	$0.213^{+0.047+0.044+0.008}_{-0.036-0.044-0.008}$	$0.419^{+0.089+0.019+0.005}_{-0.067-0.018-0.005}$
$W^-b\bar{b}$	$0.126^{+0.028+0.024+0.006}_{-0.021-0.024-0.006}$	$0.239^{+0.049+0.010+0.003}_{-0.037-0.011-0.003}$
Total $Wb\bar{b}$	$0.247^{+0.055+0.050+0.010}_{-0.042-0.050-0.010}$	$0.482^{+0.102+0.021+0.006}_{-0.077-0.021-0.006}$

Table 4. NLO QCD predictions that are obtained with different PDFs for $W^+b\bar{b}$ *and* $W^-b\bar{b}$ production channels at $\sqrt{s}$ = 14, 27 and 100 TeV. All results are in the units of pb.

Production Channel	Energy (TeV)	NNPDF3.1PDF	CT14 PDF	MSTW2008 PDF	MMHT2014 PDF	HERA PDF
$W^+b\bar{b}$	14	0.996	0.980	1.021	1.025	0.986
	27	2.059	2.025	2.105	2.119	2.096
	100	7.676	7.536	7.872	7.907	8.056
$W^-b\bar{b}$	14	0.670	0.655	0.701	0.693	0.680
	27	1.582	1.556	1.653	1.641	1.631
	100	6.972	6.839	7.216	7.190	7.319

Table 5. LO and NLO QCD predictions at $\sqrt{s}$ = 14, 27 and 100 TeV for $W^+b\bar{b}$ *and* $W^-b\bar{b}$ production channels. The uncertainties are respectively scale, α_S, and PDF errors. All results are in the units of pb.

Production Channel	Energy (TeV)	LO	NLO
$W^+b\bar{b}$	14	$0.392^{+0.079+0.086+0.015}_{-0.053-0.086-0.015}$	$0.996^{+0.226+0.046+0.008}_{-0.163-0.047-0.008}$
	27	$0.650^{+0.078+0.154+0.022}_{-0.067-0.154-0.022}$	$2.059^{+0.441+0.102+0.011}_{-0.321-0.094-0.011}$
	100	$1.713^{+0.033+0.497+0.046}_{-0.048-0.497-0.046}$	$7.676^{+1.162+0.404+0.053}_{-0.950-0.367-0.053}$
$W^-b\bar{b}$	14	$0.276^{+0.046+0.059+0.012}_{-0.037-0.059-0.012}$	$0.670^{+0.144+0.032+0.005}_{-0.105-0.031-0.005}$
	27	$0.520^{+0.060+0.123+0.018}_{-0.053-0.123-0.018}$	$1.582^{+0.318+0.075+0.008}_{-0.235-0.073-0.008}$
	100	$1.589^{+0.024+0.476+0.044}_{-0.042-0.476-0.044}$	$6.972^{+1.006+0.351+0.045}_{-0.837-0.345-0.045}$

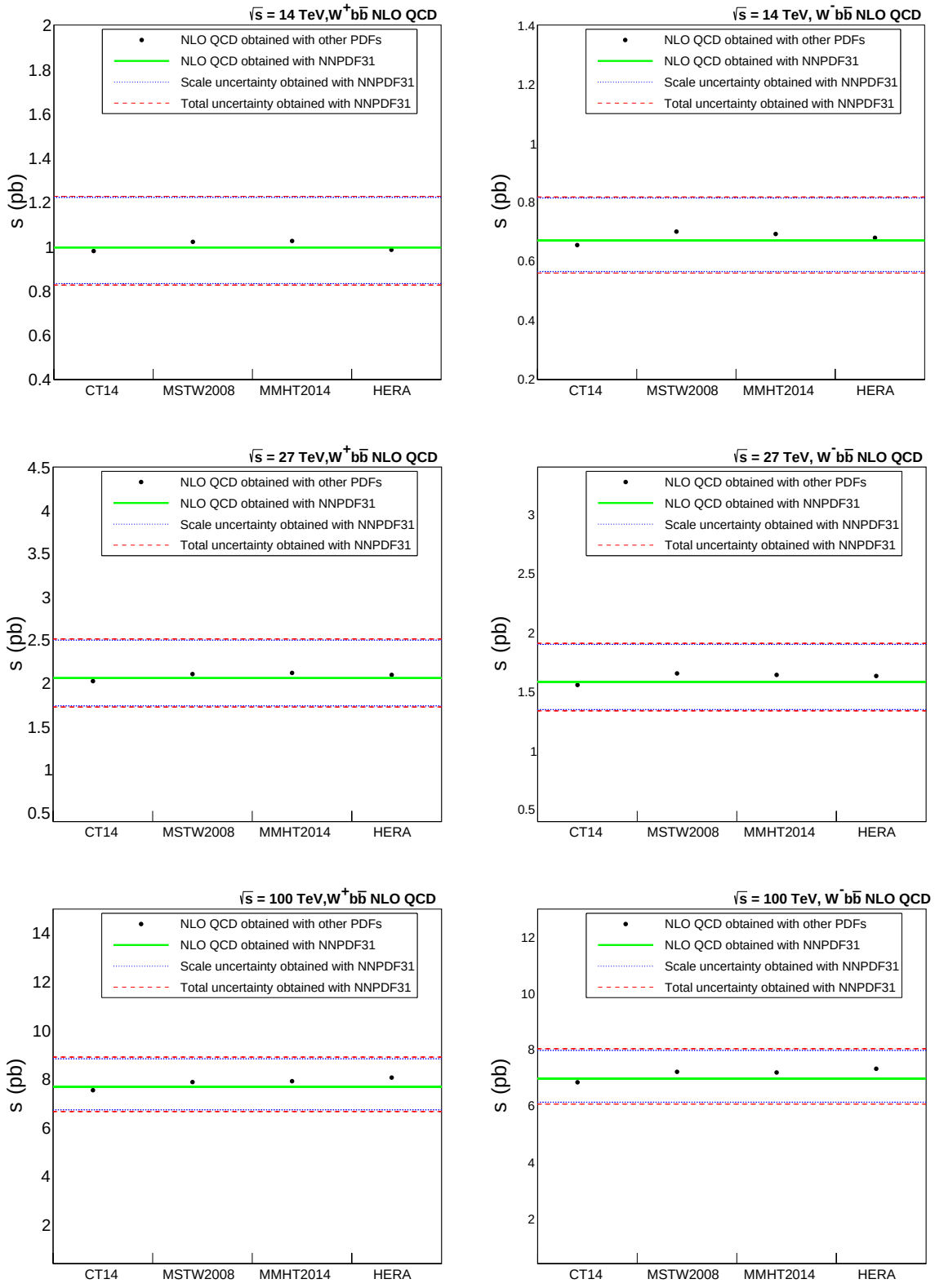

Figure 3. A comparison of NLO QCD results obtained by NNPDF3.1 with the NLO QCD results obtained by CT14, MSTW2008, MMHT2014 and HERA PDFs.

After the confirmation of the codes and the PDF set, LO and NLO QCD corrections at $\sqrt{s}$ = 14, 27 and 100 TeV have been calculated. During the calculation, LO corrections have been calculated with the LO PDF and NLO corrections have been calculated with NLO PDF. Table 5 shows the numerical results of these corrections. NLO QCD has more yield than the LO QCD for all selected energies shown in the table. For $\sqrt{s}$ = 14, 27 and 100 TeV energies of $W^+b\bar{b}$ ($W^-b\bar{b}$) channel, NLO results are respectively 2.541, 3.168 and 4.481 (2.428, 3.042 and 4.388) times higher than the LO results. Figure 4 shows this difference between LO and NLO corrections. The difference between LO and NLO QCD results increases while the energy increases. However, this

increase is not identical for both channels ($W^+b\bar{b}$ and $W^-b\bar{b}$). When the energy ranges from 14 TeV to 100 TeV, the gap between LO and NLO corrections in $W^+b\bar{b}$ channel becomes larger than the gap between LO and NLO corrections in $W^-b\bar{b}$ channel. Due to the proportionality of the cross-section and the number of events, the results in the table also show that there will be more $W^+b\bar{b}$ events than $W^-b\bar{b}$ events in the future experiments. However, the number of $W^-b\bar{b}$ events will be close to $W^+b\bar{b}$ events while the energy is increased. This is because the asymmetry between W^+ and W^- events decreases with the increasing energy.

In a collision, the number of events is proportional to the cross section and the relationship between them is given with the following equation:

$$N=\sigma \times L \quad (1)$$

where N is the number of events, σ is the cross section and L is the luminosity. This equation shows that equal amount of data at different energies provides more signal events at the highest energy. If the same number of events are taken at different energies, the highest energy will provide less amount of data to reach the same statistic with the lower energies. Based on this consideration, the following equation can be written:

$$\sigma_1 L_1 = \sigma_2 L_2 \Rightarrow L_2 = \frac{\sigma_1 L_1}{\sigma_2} \quad (2)$$

Using this equation, the following statistics are calculated at $\sqrt{s}$ = 14, 27 and 100 TeV for the required data to reach the same statistics at $\sqrt{s}$ = 7 TeV. The recorded CMS data at $\sqrt{s}$ = 7 TeV is equal to 5.55 fb^{-1}.

$$L_{14TeV} = \frac{\sigma_{7TeV} L_{7TeV}}{\sigma_{14TeV}} = \frac{0.482x5.55}{1.200} = 2.230\ fb^{-1} \quad (3)$$

$$L_{27TeV} = \frac{\sigma_{7TeV} L_{7TeV}}{\sigma_{27TeV}} = \frac{0.482x5.55}{2.597} = 1.030\ fb^{-1} \quad (4)$$

$$L_{100TeV} = \frac{\sigma_{7TeV} L_{7TeV}}{\sigma_{100TeV}} = \frac{0.482x5.55}{10.370} = 0.260\ fb^{-1} \quad (5)$$

The results in equations 3, 4 and 5 show that the required data at $\sqrt{s}$ = 14, 27 and 100 TeV are 60%, 81% and 95% less than the data at $\sqrt{s}$ = 7 TeV. Figure 5 shows the amount of data taken at different energies to reach the same statistic with the lowest energy of the LHC (7 TeV). For the future pp collision runs, the collisions at $\sqrt{s}$ = 14, 27 and 100 TeV will need less data to reach the same statistic with $\sqrt{s}$ = 7 TeV pp collision energy.

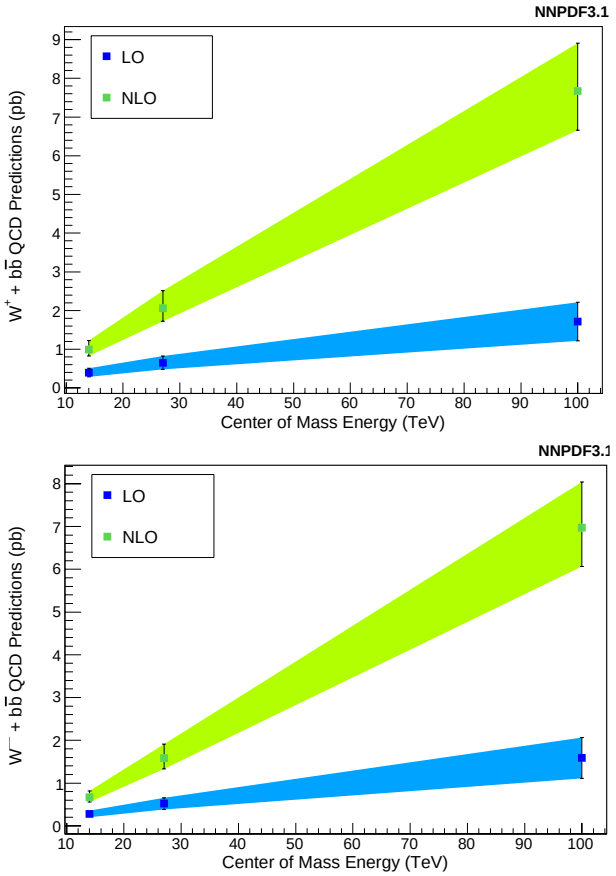

Figure 4. LO and NLO QCD predictions at $\sqrt{s}$ = 14, 27 and 100 TeV for $W^+b\bar{b}$ (top) and $W^-b\bar{b}$ (bottom).

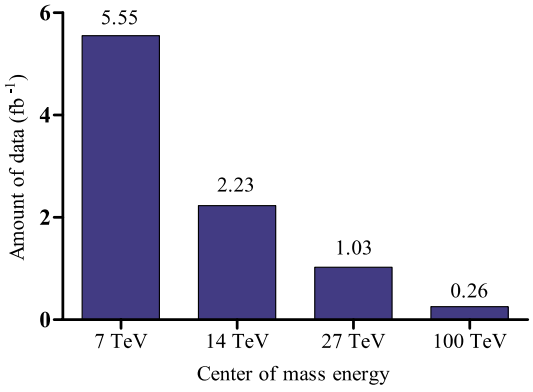

Figure 5. The required data at $\sqrt{s}$ = 14, 27 and 100 TeV to reach the same statistics with $\sqrt{s}$ = 7 TeV energy.

4. CONCLUSION

LO and NLO QCD cross sections of $W^+b\bar{b}$ and $W^-b\bar{b}$ channels at $\sqrt{s}$ = 14, 27 and 100 TeV were presented in this study. Both LO and NLO predictions were obtained by the most modern PDF, NNPDF3.1. During the calculation, the consistency of the results was confirmed by the comparison of the results with the available CMS results and the consistency of the NNPDF3.1 was confirmed via comparing with the results obtained by other PDFs. The scale uncertainties were calculated by two different methods in which different μ_R and μ_F values were specified. On the first method (scale

1), the default values of μ_R and μ_F were taken as sum of W and b quarks masses and the μ_R and μ_F values were changed as half and twice of this default value. On the second method (scale 2), the default values of μ_R and μ_F were set to W boson mass; then, the μ_R and $\mu_F$values were changed as half and twice of this default value. Following that, the scale uncertainties for both methods were calculated taking the difference between the default and changed values. The results of scale 1 were partially found to be lower than that of the scale 2. Therefore, scale 1 results were taken into account at the uncertainty results of the final LO and NLO QCD results at $\sqrt{s}$ = 14, 27 and 100 TeV. In addition to the scale uncertainty, the effect of the increasing energy on the uncertainties was analyzed by comparing energy with the scale, PDF and α_S uncertainties. Finally, using NNPDF3.1 as a reference PDF model, LO and NLO QCD predictions were obtained for the next run of the LHC (14 TeV), HE-LHC (27 TeV) and FCC-hh (100 TeV). According to the obtained results, LO and NLO QCD predictions increase as the collision energy increases. This showed that there would be more amount of data at the next LHC run and FCC runs and the necessary amount of data to reach same statistics with the data at $\sqrt{s}$ = 7 TeV would respectively reduce while the collision energy was increased to $\sqrt{s}$ = 14, 27 and 100 TeV.

Acknowledgement

The numerical calculations reported in this paper were fully/partially performed at TUBITAK ULAKBIM, High Performance and Grid Computing Center (TRUBA resources).

REFERENCES

[1] Evans L, Bryant P. LHC Machine. Journal of Instrumentation 2008; 3: S08001.

[2] Kuehn S. Impact of the HL-LHC detector upgrades on the physics program. International Workshop on Future Linear Colliders. LCWS2021. Zurich, 15-18 March 2021.

[3] Future Circular Collider Conceptual Design Report, The European Organization for Nuclear Research, (2019), URL:https://fcc-cdr.web.cern.ch/

[4] The FCC Collaboration, Eur. Phys. J Spec. Top. 2019;228:261-623.

[5] Abada A, Abrescia M, Abdussalam S, Abdyukhanov I, Fernandez J, Abramov A, et al. HE-LHC: The High Energy Large Hadron Collider. Eur. Phys. J. Spec. Top. 2019; 228:1109–1382.

[6] The FCC Collaboration. FCC-hh: The Hadron Collider: Future Circular Collider Conceptual Design Report Volume 3. Eur. Phys. J. Spec. Top. 2019; 228:755–1107.

[7] Campbell J, Ellis K, Neumann T, Williams C. MCFM Monte Carlo for FeMtobarn processes. [2022 November 3] Available from: https://mcfm.fnal.gov/

[8] Buckley A, Ferrando J, Lloyd S, Nordstrom K, Page B, Ruefenacht M, et al. LHAPDF6: parton density access in the LHC precision era. Eur. Phys. J. C. 2015; 75(132): 1-20.

[9] Cordero F, Reina L, Wackeroth D. W and Z boson production with a massive bottom quark pair at the Large Hadron Collider. Phys. Rev. D 2009; 80: 034015.

[10] Catani S, Dokshitzer YL, Webber BR. The k_T clustering algorithm for jets in deep inelastic scattering and hadron collisions. Phys. Lett. B. 1992; 285 (3): 291-299.

[11] Kilgore B, Giele T. Next-to-leading order gluonic three-jet production at hadron colliders. Phys. Rev. D. 1997; 55:7183.

[12] Dilsiz K, Tiras E. Inclusive W boson QCD predictions and lepton charge asymmetry in proton-proton collisions at $\sqrt{s}$ = 14 TeV. Canadian J. of Phys. 2018; 96(9):1029-1033.

[13] Ball R, Bertone V, Carrazza S, Debbio L, Forte S, Groth-Merrild P, et al. Parton distributions from high-precision collider data. Eur. Phys. J. C. 2017; 77(10): 663.

[14] Chatrchyan S, Khachatryan V, Sirunyan A, Tumasyan A, Adam W, Bergauer W, et al. Measurement of the production cross section for a W boson and two b jets in pp collisions at $\sqrt{s}$ = 7 TeV. Phys. Lett. B. 2014; 735: 204–225.

[15] Dulat S, Hou T, Gao J, Guzzi M, Huston J, Nadolsky P, et al. New parton distribution functions from a global analysis of quantum chromodynamics. Phys. Rev. D. 2016; 93(3): 033006.

[16] Martin A, Stirling S, Throne RS, Watt G. Parton distributions for the LHC. Eur. Phys. J. C. 2009; 63:189–285.

[17] Martin A, Stirling S, Thorne RS, Watt G. Heavy-quark mass dependence in global PDF analyses and 3 and 4 flavour parton distributions. Eur. Phys. J. C. 2010; 70: 51–72.

[18] Harland-Lang L.A, Martin A.D, Motylinski P, Throne R.S. Parton distributions in the LHC era:MMHT 2014 PDFs. Eur. Phys. J. C. 2015;75(5): 204.

[19] Abramowicz H, Abt I, Adamczyk L, Adamus M, Andreev V, Antonelli S, et al. Combination of measurements of inclusive deep inelastic $e^{\pm}$ p scattering cross section and QCD analysis of HERA data. Eur. Phys. J. C. 2015; 75:580.

[20] Butterworth J, Carrazza S, Cooper-Sarkar A, Roeck A, Feltesse J, Forte S, et al. PDF4LHC recommendations for LHC Run II. J. Phys. G. 2016; 43: 023001.